

## Mathematical Models of Within-Host and Transmission Dynamics to Determine Effects of Malaria Interventions in a Variety of Transmission Settings

Philip Eckhoff\*

Intellectual Ventures Laboratory, Bellevue, Washington

**Abstract.** A model for *Anopheles* population dynamics and malaria transmission is combined with a within-host dynamics microsolver to study baseline transmission, the effects of seasonality, and the impact of interventions. The Garki Project is recreated in simulation of the pre-intervention baseline and the different combinations of interventions deployed. Modifications are introduced, and longer project duration, extension of dry-season spraying, and transmission-blocking vaccines together achieve local elimination in some conditions. A variety of interventions are simulated in transmission settings that vary in transmission intensity and underlying seasonality. Adding vaccines to existing vector control efforts extends the ability to achieve elimination to higher baseline transmission and less favorable vector behavior. If one species of the *Anopheles gambiae* species complex feeds disproportionately outdoors for a given complex average behavior, vector control impacts are less than for a single species. Non-zero dry-season transmission limits seasonal oscillation in parasite dynamics and impact of wet-season interventions.

### INTRODUCTION

In October 2007, a renewed effort towards the global eradication of malaria was announced to reduce the high burden of malaria<sup>1,2</sup> permanently to zero. Malaria exhibits a diverse set of epidemiologic settings, with varied baseline transmission intensities,<sup>3</sup> strength of seasonality, diverse local combinations of vector species,<sup>4</sup> and human heterogeneities, such as housing conditions and disorders of the erythrocyte. As a result of these geographic and demographic heterogeneities, different locations will require different strategies to interrupt transmission. A variety of vector control tools ranging from insecticide-treated nets (ITNs)<sup>5,6</sup> to indoor residual spraying (IRS)<sup>7,8</sup> to larval habitat modification or larvicides<sup>9–11</sup> are available to public health programs. The response of the local malaria transmission patterns to deployed interventions depends on the mixture of vector species and their individual ecologies and behaviors, and the mixture can change in response to deployed interventions.<sup>5,12–14</sup> Insecticide-treated nets and IRS are powerful tools against indoor feeding and resting mosquitoes, but nets do not stop feeds that occur outdoors or earlier in the evening, and spraying does not kill mosquitoes that do not rest indoors. Drug distribution through mass drug administration (MDA) or mass screen-and-treat campaigns can have strong impacts on parasite levels at least temporarily,<sup>15–19</sup> but many modes of drug distribution are limited by difficulties of achieving high coverage frequently. Finally, vaccines under development are only partially efficacious and will most likely require high coverage as a result.<sup>20,21</sup> Vaccines also require close study of the cost and time course of efficacy. The extent and durability of gains achieved through drug distribution or vaccine deployment will depend critically on the baseline intensity of transmission, with highest impact on transmission seen primarily at low baseline transmission or low transmission levels achieved through vector control. Thus, higher-transmission settings will most likely require layers of interventions limiting the parasite at many different points in the transmission cycle. New

interventions targeting other portions of the vector or parasite life cycles may also be required.<sup>22–25</sup>

Design of such combined strategies will benefit from computer-based modeling to explore the many possible dimensions of coverage, frequency of distribution, and portfolio of tools. Mathematical models helped inform the use of vector control in the first global eradication program.<sup>26–29</sup> These models were an important step forward in the application of mathematical formulations to public health, but the impact of assumptions and sensitivities to vector behavior and ecology was not recognized at the outset and led to overly optimistic projections.<sup>29</sup> A new mathematical model was built to analyze the results and implementation of the Garki Project,<sup>7</sup> and this model provided the basis of an entire new generation of malaria models. These models recognized more of the complexities of malaria transmission including multiple local vector species with different ecology and behavior. As a result, interpretations of model outputs were more measured and cautious. Recent models for strategy evaluation have focused on local vector dynamics<sup>30,31</sup> and integrated vector control,<sup>9,24,25</sup> anti-malarial drugs,<sup>15,32–34</sup> MDA, mass screen-and-treat, and new modes of drug distribution such as intermittent preventative treatment,<sup>35</sup> potential vaccines,<sup>20,36–38</sup> and integrated intervention strategies that use tools from multiple categories.<sup>23,24,39,40</sup> Mathematical models can also help explore the potential impact of new tools proposed or under development. Such expansion and use of modeling is a vital component of the MalERA research agenda.<sup>41,42</sup> Applying multiple models to the same question appears to be a powerful path forward and is enabled by ensemble modeling.<sup>43</sup>

This report presents a new model combining detailed vector population dynamics and interactions with the human population<sup>44</sup> with a microsimulation for human immunity and within-host parasite dynamics.<sup>45</sup> The present model builds on the work of Macdonald,<sup>27</sup> the Garki model,<sup>7</sup> and modern malaria modeling efforts<sup>23,39,40,46</sup> to model multiple vector species simultaneously interacting with a human population. Each species can respond separately to interventions, and the model can thus track the changing ratio of burden of transmission by species. This work builds on the earlier vector model and now includes a detailed parasite dynamics microsolver to enable tracking of detected parasite levels and simulation of the impact of drug programs. Models for

\*Address correspondence to Philip Eckhoff, Intellectual Ventures Laboratory, 1575 132nd Avenue NE, Bellevue, WA 98004. E-mail: peckhoff@intven.com

available interventions such as ITNs and IRS are presented and then deployed within simulations for a variety of transmission settings with different transmission intensities, vector behaviors, and seasonality-driven ecologies.

The baseline and intervention coverage dynamics of the Garki Project<sup>7</sup> are replicated in simulation as a validation. The Garki Project interval is then extended and implemented with different intervention implementations and potential new tools. The potential profiles of new tools such as pre-erythrocytic vaccines, which act to prevent blood-stage infection through action at the sporozoite or liver stage, and gametocyte-blocking or transmission-blocking vaccines, which limit transmission from humans to mosquitoes, are evaluated for impact in different transmission settings with and without concurrent vector control through IRS. The relationships among transmission setting, baseline transmission intensity, vector ecology and behavior, and intervention characteristics are explored.

## MATERIALS AND METHODS

**Model structure overview.** The model for vector population dynamics with a human agent-based framework presented in the report by the author<sup>44</sup> is simulated with simple and detailed microsolvers for infections in the simulated human agents. For the simple human infection model, infections are represented by an exponentially-distributed duration of constant infectiousness. Most simulations presented implement a detailed microsolver for the immune and parasite dynamics for each person<sup>45</sup> unless it is explicitly stated that a simulation uses the simple infection model. Intervention-free vector dynamics are fit to baseline entomologic inoculation rate (EIR) data for multiple settings including Namawala, Tanzania<sup>47</sup> and multiple sites for the Garki Project.<sup>7</sup> Once these baseline vector population dynamics are constructed as described in a parallel paper,<sup>48</sup> various combinations of intervention distributions are introduced in simulations, and these combinations are referred to as campaigns in the model and the report. Each campaign is composed of at least one intervention distribution event, although most realistic campaigns will be composed of multiple intervention components repeated at intervals. Each intervention distribution event has a schedule that specifies the start timing and the duration of each distribution, and the number and frequency of repetition. Each event also specifies the target demographic (infants, children, mothers, general population) and coverage. Each component of the model is described below, including the vector transmission dynamics, within-host parasite dynamics, and interventions. Summaries of the parameterization and calibration processes are also provided.

**Vector transmission model.** The mosquito feeding cycle detailed in the report by the author<sup>44</sup> is responsible for tracking intervention-imposed mosquito mortality, as well as all transmission from mosquitoes to humans and back. The model must support multiple simultaneous interventions for each person, such as ITNs and IRS, or house screening and IRS. To accomplish this feature, the calculation of feeding cycle outcomes is constructed as a series of binary choices, so that the effect on overall outcomes is conditional on arriving at that choice. For example, a mosquito attempting a blood feed will first select the type of host, whether human or animal.

Because the probability of this choice will depend on the behavior of the given species, the remaining outcomes are thus conditional on mosquito host selection behavior. For human feeds, the next choice is indoor or outdoor, again depending on species preferences and propensities. The indoor feeding rate, or endophagy, parameter used in simulations describes the proportion of human feeds that occur indoors as a proportion of all human feeds.<sup>49,50</sup> The effects of interventions are included in the order that they would be experienced by a mosquito: for example, screening reduces the probability of finding a human host indoors, which reduces the overall probability of feeding on that specific host, which reduces the probability of dying from IRS post-feeding inside that house. The outcomes for each human are gathered into a discrete probability measure across the entire human population of outcomes such as successful feed, dying post-feed, inability to find a host, and dying pre-feed, optionally weighting by the heterogeneous biting for each human. All feeding mosquitoes can thus be sorted into outcomes depending on the choice of host and location of feed, along with all the interventions associated with a given host. The detailed probability equations for each collected and categorized outcome are provided in the report of the author.<sup>44</sup> Individual humans can own vector control interventions, receive drug treatments and regimens, or be administered vaccines with defined modes of action such as pre-erythrocytic (acting to stop an infection before the blood-stage) or gametocyte-blocking/transmission-blocking (acting to stop the infected human from transmitting infection to the mosquito), specified efficacies, and customizable durations of effect.

The sequential nature of intervention actions within the binary choice structure enables a single intervention to have multiple effects such as deterrence and toxicity and enables multiple interventions to be combined in protection of a single person. In the modified cohort version of the model described by previously,<sup>44</sup> those mosquitoes that are deterred from feeding remain in the cohort and have a chance to feed in the following time step. The more deterred feeds, the fewer completed feeds will occur per mosquito during the incubation period, and the average resulting oviposition interval is lengthened. In addition, as the mosquitoes feeding in the following time step are again distributed across the human population at random, successful feeds will be concentrated on those humans who are not protected by deterring interventions. However, because the cohort model has a certain fraction of all mosquitoes in each cohort attempting to feed at each time step, both these effects of deterred feeds may be underestimated in magnitude. This same vector model can be run with each mosquito represented by an individual agent for additional computational cost. In this version, an oviposition timer is added as a variable to each mosquito agent and is set to the oviposition interval upon a successful feed. Once the time runs out, the mosquito lays eggs and resumes host seeking. If a feed is deterred, the mosquito automatically attempts to feed in the following time step, rather than just a fractional probability in the cohort model. The individual mosquito version of the model can thus capture both of these effects of deterrence at a level closer to reality.

**Within-host parasite dynamics.** Once a person receives a new infection, the within-host parasite dynamics are governed by the microsolver with detailed parasite and immune interactions.<sup>45</sup> This microsolver uses a combination of discrete

events and continuous processes to represent the parasite development and immune response. The infection begins with a fixed seven-day latency in the liver, and after the infection-specific timer expires, the liver schizonts rupture to release merozoites and start the blood stage of the infection. The counts of parasites by expressed surface antigen are tracked for each infection, and each infection has a repertoire of 50 *Plasmodium falciparum* erythrocyte membrane protein-1 (PFEMP-1) variants. Each infection also has a set of minor antigenic epitopes<sup>51</sup> and a specific merozoite antigen.<sup>52</sup> The within-host dynamics are simulated with a one-hour time step, and a 48-hour timer governs each asexual cycle. During a cycle, innate immune responses are stimulated and specific antibody responses build to each antigen present, and the innate and specific immune responses clear parasites. When the asexual timer expires, the infected erythrocyte schizonts rupture and release merozoites to create the next generation of infected erythrocytes. Antigenic switching occurs as new variants are introduced from the available repertoire. As specific adapted immune responses develop, the original variants are cleared, and once an infection fails to introduce a new variant, the infection will soon be cleared. Superinfection is supported, and each infection draws its set of 50 PfEMP-1 variants, its set of 5 minor epitopes, and its merozoite antigen from the overall simulation parasite population of available variants. Results are shown for a variety of parasite antigenic diversity levels. Full detailed equations for the microsolver are available,<sup>45</sup> as well as the effects of varying parasite antigenic diversity levels in each location.<sup>48</sup>

**Intervention effects.** Each intervention distributed can have multiple effects and durability constants. Within the model, an ITN has an input efficacy parameter associated with successfully blocking an attempted feed, and another input efficacy parameter for killing the mosquito conditional on blocking the feed. The model does not capture any impact of delayed killing by an ITN without blocking the feed. Because each of these efficacies can also have a defined durability, the user can specify the duration of the insecticide killing effect and the duration of the feed-blocking effect. Blocked feeds result in the vector attempting to feed again the next time step instead of experiencing a gonotrophic latency and laying eggs as after a successful feed. Thus, blocking without toxicity could actually increase the biting rates experienced by non-protected persons in certain regimens. Different possible temporal profiles for intervention efficacy are simulated to observe the impact of this structural assumption. These profiles include constant efficacy for a specified duration followed by a decrease to zero efficacy (fixed-box), exponential decay from an initial specified efficacy to zero with a specified decay time constant (exponential decay), or a fixed interval of constant efficacy at the initial value followed by an exponential decay to zero with a second time constant (box-decay). The box-decay pattern would represent a decaying insecticide concentration or antibody titer that retained its maximum effect above a given threshold. The two effects of IRS consist of repellency pre-feed or mortality post-feed, and separate time constants can be placed on the temporal profile of each of these. Efficacies for ITNs and IRS in the context of the present vector-feeding model are tuned to approximate the consensus impact at the population level.<sup>53,54</sup> Physical durability of distributed ITNs is an uncertain parameter, and the effects of these uncertainties are explored in the Results.

Potential vaccines modeled include pre-erythrocytic vaccines (PEVs), which reduce the actual force of infection from the mosquito bites experience by a vaccinated person, and gametocyte-blocking or sexual-stage transmission-blocking vaccines (TBVs), which reduce the probability of an infectious person infecting a mosquito. Potential therapeutic blood-stage vaccines have not yet been incorporated into the model. Efficacy for a PEV in the context of this simulation is defined as the reduction in inoculations with potential to create infections experienced by an individual in a given time step; a 50% effective vaccine in the simulation means that a protected person will have their liver challenged by half as many effective inoculations. Because the model includes a saturation of the number of simultaneous infections for an individual, this feature creates a saturating, non-linear relationship between EIR and force of infection.<sup>55</sup> As such, this does not necessarily correspond to a 50% reduction in number of experienced infections. The reduction in new infections will more closely track the reduction in effective inoculations at lower transmission levels. At high transmission levels, there may not be much difference in the human epidemiology as a result. Efficacy for a TBV is defined in the model as the reduction in probability that a mosquito feeding on an infected human will become infected itself. Vaccine efficacy starts at the specified efficacy and can evolve over time in either the exponential decay, constant effect for fixed duration, or box-decay patterns. Vaccines in this paper are hypothetical in efficacy and durability and are intended to map out the impacts as a function of parameter space.

**Local simulation construction.** The basic vector model that was parameterized for Namawala<sup>44,47</sup> is retained, but new locations such as Garki require fitting to be properly parameterized. Local vector bionomic and behavioral data are used where available, and if not available, best known values for the species in general are used. Weather for the site is an input to the model, and the synthetic population is constructed with appropriate population sizes by age. The overall larval carrying capacity scalar for each species is then adjusted iteratively in simulation runs to match local human biting rate data. Construction of baseline simulations for Namawala and Garki is described in another report,<sup>48</sup> which also explores the effects of available antigenic variants in the overall parasite population and the corresponding effect on age prevalence. Once a local setting is parameterized, the transmission level can be adjusted up and down while maintaining species abundance ratios by scaling all larval habitat values equally. The impact of routine case management on transmission is ignored in constructing baselines at present, and these effects will be incorporated into future modeling studies. Simulations described as Namawala have an annual EIR by species corresponding to Namawala and approximately matched temporal profiles. Simulations described as Namawala  $\times$  0.1 have the same ratio of species and temporal profile as Namawala, but vector populations will be a factor of 10 lower for each species. This feature enables an investigation of the impact of transmission intensity, holding species ratios, and seasonality constant. As described in another report,<sup>45</sup> the within-host parasite model uses known values for some parameters such as merozoites per schizont. Other parameters are constrained so that simulated infections match cumulative outcomes in the malariatherapy data<sup>56</sup> for measured durations of infections, peak parasite densities, the decrease

in parasite densities over time, and the interval between peaks. The antigenic switching rate<sup>57</sup> is more difficult to constrain, and evolutionary arguments were used in its parameterization. The number of antigenic variants in the overall parasite population is set to match the age-prevalence curves from Namawala<sup>58</sup> and Garki.<sup>7</sup>

Many simulations are run for each scenario and set of parameters, and mean and variance are presented for the trajectories of interest. Generation of this stochastic ensemble for a single condition enables presentation of intrinsic stochastic variability. Variation of intervention coverage and efficacy across scenarios demonstrates the translation of uncertainty in these parameters to output measures of impact. Sensitivity of results to input data such as vector population sizes and behavior are also calculated. In addition, multi-dimensional parameters sweeps can be used to construct plots showing the change in the probability of local elimination (or some other defined event) as an empirical function of the parameters of interest.

## RESULTS

**Garki Project reconstruction and extension.** The Garki District baseline vector and parasite dynamics and the impact of interventions as implemented are first recreated in simulation as a validation. The Garki Project<sup>7</sup> used IRS and MDA to study the impact of large-scale campaigns in high-transmission settings. The project was well-instrumented, collecting weather, human demographic, entomologic, and parasitologic data longitudinally leading up to, during, and after the project. Some villages did not receive any interventions as a control, others repeated applications of propoxur during the rainy season, and a third set received MDA every ten weeks. The interventions lasted for two rainy seasons and the intervening dry season, and distribution of interventions was ceased after 18 months without definitively clearing the human parasite reservoir, although some villages experienced weeks without human detected parasites. A mathematical model was built to explore and understand the results of the project,<sup>7</sup> and many essential features, such as the mixture of local vector species, were captured. The Garki Project, its impacts, and possible variations on its implementation can be studied with the present vector transmission model,<sup>44</sup> with vector population dynamics driven by historical Garki weather and with local vector population characteristics.

The vector model is coupled to the detailed model of within-host parasite dynamics with full antigenic variation, and lower parasite population diversity (4 available merozoite antigenic variants, 4 available sets of 5 minor epitopes, and 300 available PfEMP-1 variants), and a corresponding level for immunologic memory of 0.225 on the non-dimensional antibody scale.<sup>45,48</sup> This parameter combination matches population averages of detected parasitemia and is computationally faster than other parameterizations for this microsolver. Reconstruction of the Garki Project outcomes for baseline, IRS only, IRS and MDA, and then IRS and MDA combined with a 50% effective TBV are shown in Figure 1. The IRS campaigns in this simulation cover 90% of the population for six months starting just before the beginning of each rainy season. Each feed on a person in a treated house is modeled to have a 60% chance of post-feeding mortality. Model implementation of MDA gives a full course of treat-

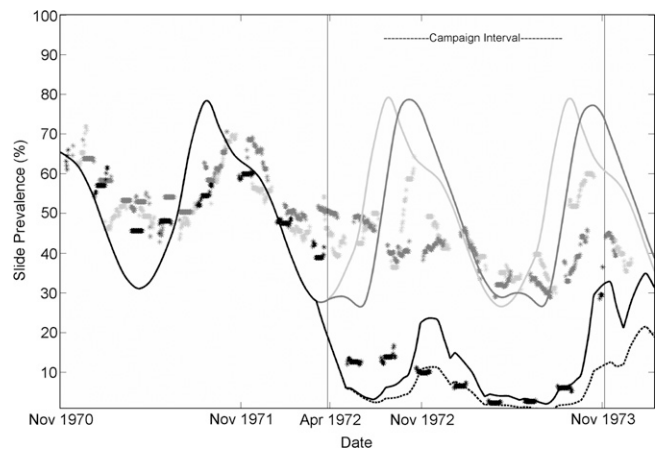


FIGURE 1. Reconstruction of the Garki Project outcomes with the detailed mechanistic within-host model and vector dynamics modeled after Garki. Light gray is baseline, then indoor residual spraying (IRS) in dark gray, then IRS plus mass drug administration in black. The dotted black line shows the potential impact of overlaying the IRS plus mass drug administration campaign with mass distribution of a sexual-stage transmission-blocking vaccine with 50% efficacy at reducing transmission from humans to mosquitoes.

ment to a random 80% of the population at eight-week intervals. A full course of drugs results in approximately five weeks of increased parasite mortality in the detailed parasite microsolver because drugs are modeled as increased asexual stage mortality rather than absolute prophylaxis. The distributed TBV is mass-distributed to 90% of all persons, with a 50% initial efficacy exponentially decaying with a four-year time constant. These traces can be compared with data from the Garki Project for each category of village<sup>7,59</sup> plotted as smoothed point data.

Because the Garki Project was unable to interrupt transmission and clear the human parasite reservoir, it is of interest to investigate possible perturbations and modifications of the original campaign and to understand the system effects that maintained transmission as the project was conducted. Simulations can explore the potential impact of new tools, longer campaign durations, and different deployment timings and coverages. The final trace (black dashes) in Figure 1 shows the impact of a 50% effective TBV with a decay time constant of four years distributed to 90% of the population in the IRS and MDA villages. Parasitemia and transmission are even further reduced, but elimination remains elusive. The same traces with two additional modifications are shown in Figure 2: the post-indoor-feed killing efficacy caused by IRS spraying rounds now begins one month before the start of the rainy season and is extended one month further into the dry season for a total of eight months per year. A more pronounced decrease in detected prevalence is observed by limiting the tail of transmission into the dry season. Finally, the intervention period of the project is extended to 36 months instead of the original 18 months. The MDA distributions occur periodically for 36 months instead of 18 months, IRS occurs around 3 rainy seasons instead of only 2 rainy seasons, and an additional mass distribution of TBV is added at 18 months. With the spraying in the dry season, an extended-duration program, and new tools such as a TBV, elimination is achieved in the IRS plus MDA plus TBV trace (black dashes) in Figure 2.

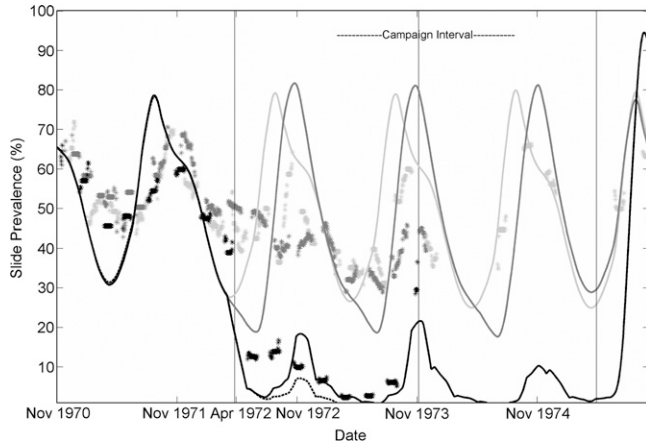


FIGURE 2. Modification of the Garki Project campaign, extending the overall campaign duration to 36 months and with spray campaigns scheduled to maintain indoor residual spraying (IRS) efficacy over a window from one month before the rainy season until one month into the dry season. For the propoxur campaign used in Garki, this would require an additional spray round in the dry season leading into the rainy season. Light gray is baseline, then IRS in dark gray, then IRS plus mass drug administration in black. The dotted black line shows the potential impact of adding mass distribution of a sexual-stage vaccine with 50% efficacy to the IRS plus mass drug administration campaign.

**Effect of vector-feeding behavior.** It is important to understand how the baseline transmission intensity and vector-feeding behavior and ecology will impact intervention outcomes. To investigate these effects, the well-parameterized vector population dynamics for Namawala are used as the basis for simulations. Baseline dynamics and the effects of simulated IRS campaigns are shown for Namawala in Figure 3A and B, and a 0.1 scaling of Namawala vector populations is shown in Figure 3C and D. Parasite population diversity is now increased to 100 merozoite, 100 minor epitopes, and 1,000 PfEMP-1 variants, and the immunologic memory is set to 0.3. Each new infection will draw one merozoite antigen from the set of 100, 5 minor epitopes from the set of 100, and 50 PfEMP-1 variants from the set of 1000. This combination is most accurate in not only matching population average parasitemia but also recreating measured age prevalence patterns. That additional capability compensates for the substantial increase in computational cost over the previous parameterization. The IRS campaign is run with 70% and 90% coverage and for *An. arabiensis* indoor feeding propensities of 0.47, corresponding to the proportion of *An. gambiae sensu lato* observed to rest indoors during the Garki Project<sup>7</sup> and close to the value for *An. arabiensis* observed in Dar es Salaam,<sup>60</sup> and 0.7, closer to values observed in other parts of Tanzania.<sup>61</sup> For a 70% coverage condition, 70% of houses are treated and feeds occurring inside these houses result in an 80% post-feeding mortality. Baseline dynamics for Namawala exhibit low seasonality in detected prevalence despite a strongly seasonal EIR, as observed in the field.<sup>47</sup> This finding is due to the fact that even in the low transmission season, most months in Namawala experience a cumulative monthly EIR of > 6 infectious bites. Decreasing the vector populations by a factor of 10 reduces this dry season transmission and introduces a stronger seasonal oscillation in detected prevalence. The impact of non-zero dry season transmission and hotspots

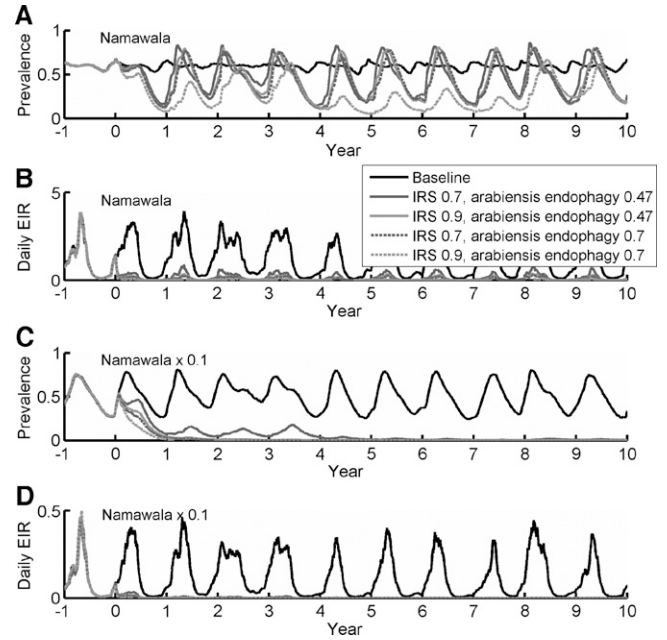


FIGURE 3. Effect of indoor residual spraying (IRS) campaigns on detected prevalence (A and C) and daily entomologic inoculation rate (EIR) (B and D). Simulations use Namawala, Tanzania weather and mixture of vector species, with (A and B) based on actual Namawala EIR and with the vector populations in (C and D) reduced to 0.1 of original values. Results are shown for two separate values of *Anopheles arabiensis* endophagy. Disease persists for all simulations in (A and B), but disease fades out in (C and D) with the exception of the 70% IRS coverage for *An. arabiensis* feeding indoors only 47% of the time.

have been studied, measured, and modeled,<sup>40,62,63</sup> and such spatial and temporal heterogeneities strongly affect the response to campaigns such as seasonal vector control and MDA.<sup>40</sup> These non-zero dry-season dynamics are especially relevant for Namawala, for which specific dry season refugia have been identified.<sup>64</sup> For Namawala, 70% IRS coverage for 0.47 and 0.7 *arabiensis* endophagy and 90% coverage for 0.47 *arabiensis* endophagy produce similar traces in prevalence, although higher indoor feeding and higher coverage drive substantial relative decreases in EIR. The 90% coverage campaign with 70% indoor feeding decreases EIR enough to drive a further decrease in prevalence, illustrating a nonlinear effect on EIR.

**Effect of *An. gambiae* species complex partition.** When building baseline simulations, it is essential to understand the impacts of model assumptions and parameter sensitivities. It is also important to understand uncertainties in available data and the impact of assumptions required to interpret available field data. The entomologic data for the Garki Project does not separate *An. gambiae sensu lato* into members of the complex, but it does report that members of the complex rested indoors after 47% of feeds. The existence of the *An. gambiae* complex was known, and later studies investigated the partition of the complex.<sup>65</sup> The existence of a component with preferentially outdoor feeding behavior was identified as a reason for the results of spray campaigns.<sup>66</sup> Simulation with individual species requires making a series of assumptions on how to partition the species complex and the indoor feeds because the proportions were not known when planning the Garki Project

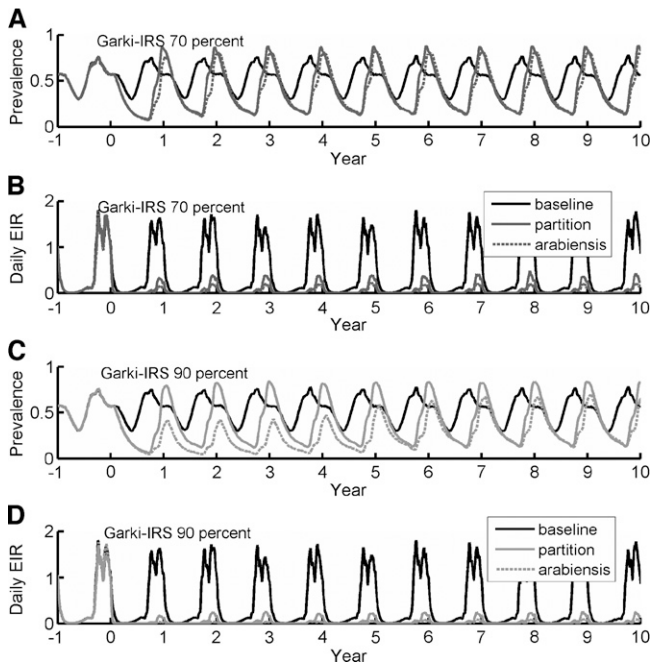


FIGURE 4. Effect of partitioning *Anopheles gambiae sensu lato* into *An. gambiae sensu stricto* and *An. arabiensis*. **A** and **B**, Effect of 70% coverage of indoor residual spraying (IRS) on detected prevalence and daily entomologic inoculation rate (EIR) for even partition of the complex into its components (solid line) and 90% dominance by *An. arabiensis* (dashed line). **C** and **D**, Simulation of campaign and the impact of *An. gambiae* complex partition are repeated for IRS with 90% coverage.

and remain unknown in many other areas of interest. Unfortunately, this choice of partition can impact entomologic and parasitologic outcomes, as shown in Figure 4. A skewed partition in which *An. arabiensis* makes up approximately 90% of the local complex and is responsible for all outdoor feeds and in which *An. gambiae sensu stricto* feeding exclusively indoors is shown in Figure 4. An alternative is to split the complex equally between *An. gambiae sensu stricto* and *An. arabiensis*. To properly account for measured outdoor feeding, *An. gambiae sensu stricto* is set to rest indoors 80% of feeds and *An. arabiensis* 20% of feeds (Figure 4: solid black line is the intervention-free scenario). The impact of a 70% coverage IRS campaign on measured prevalence and daily EIR is shown in Figure 4A and B, and the impact of repeat simulations with 90% IRS coverage are shown in Figure 4C and D. For the 70% IRS coverage condition (Figure 4A and B), substantial deviations appear in daily EIR, although discrepancies do not yet appear in prevalence. As IRS coverage increases to 90%, the difference in prevalence becomes dramatic. These deviations produce significant differences in disease fade out propensity at lower transmission intensities. Such an impact of partition makes sense because the probability of surviving four feeds with 50% mortality is 6.3%, and surviving four feeds with 25% mortality is 31.6%, which is much more than twice as high, and more than compensates for the other half of the population experiencing 75% mortality.

**Impact of vaccines.** The present model can be used to explore the potential impact of new vaccines (PEV and TBV), as has been performed in other modeling frameworks.<sup>20,23,36,40</sup> Returning to the Namawala simulation in Figure 3, several

different vaccines are introduced with different modes of action and efficacy levels. The scenario for mass vaccination is first simulated without concurrent vector control. This scenario would not be a standard rollout, but is intended to illustrate the necessity for either low transmission or combination with vector control efforts. The simulated effects in Namawala of a PEV with efficacy exponentially decaying with a four-year time constant mass distributed every two years is shown in Figure 5A and B. Baseline transmission is high enough that only minor perturbations are seen in prevalence, slightly increasing the seasonal oscillation as expected, and no discernible change occurs in EIR. For Namawala seasonality with baseline transmission scaled down by a factor of 10 (Figure 5C and D), the 90% effective PEV does produce decreases in prevalence with, in turn, reduces EIR, which can further reduce prevalence. A sexual-stage TBV with the same efficacy and duration values as the PEV above is introduced in baseline Namawala (Figure 5E and F). Minimal perturbation is observed in prevalence, but there is a clear reduction in EIR.

Because a high-efficacy vaccine had limited simulated impact at high transmission in the absence of vector control, the next simulations study the impact of rolling out vaccines on top of existing vector control activities. As described above, vectors exhibit a variety of feeding behaviors,<sup>4,67</sup> which modify the impact of interventions such as bed nets, which target indoor feeding. Baseline transmission intensity varies geographically by multiple orders of magnitude.<sup>3</sup> Parameter studies in the present model can systematically map the

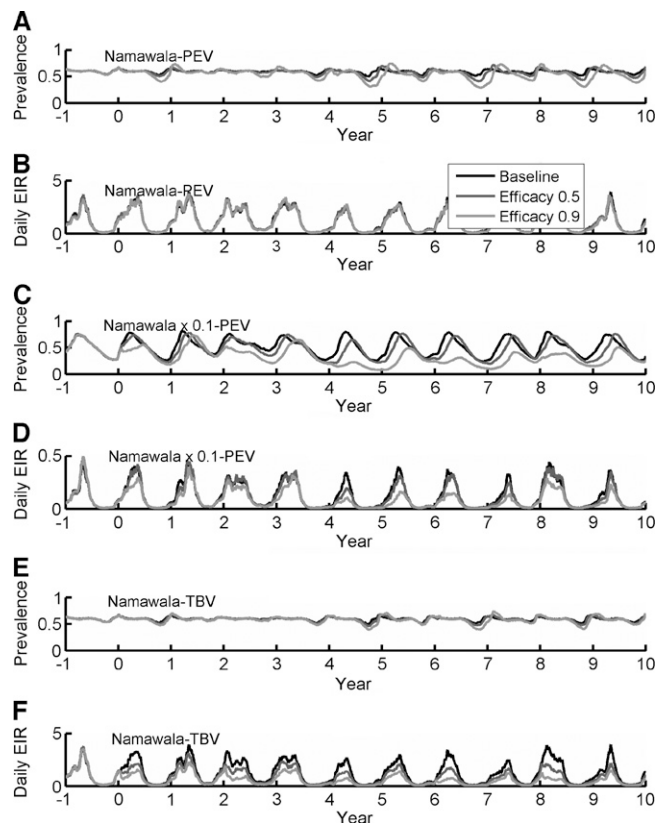


FIGURE 5. Effects on detected prevalence and daily entomologic inoculation rate induced by pre-erythrocytic (**A–D**) and sexual-stage transmission-blocking (**E** and **F**) vaccines introduced in Namawala, Tanzania (**A**, **B**, **E**, and **F**) and 0.1 Namawala intensity (**C** and **D**). PEV = pre-erythrocytic vaccine; TBV = transmission-blocking vaccine.

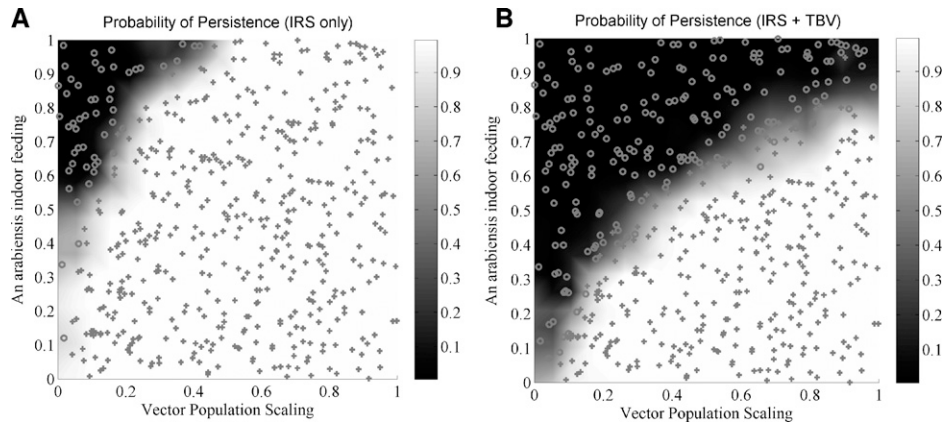


FIGURE 6. Plots of the probability of disease persistence for (A) indoor residual spraying (IRS) and (B) IRS plus a sexual-stage transmission-blocking vaccine (TBV), as a function of the indoor feeding propensity of *Anopheles arabiensis* and the scaling of the vector population. Simulations based on Namawala, Tanzania seasonality and vector composition with a simple infection model.

regions of parameter space in which existing tools can achieve desired impacts and new tools may be required. The effects of baseline transmission and the indoor feeding propensities of *An. arabiensis* are explored for two campaign designs, one with IRS only and a second with IRS and a hypothetical sexual-stage vaccine. The simulation setting, vector ratios, and seasonality are based on Namawala<sup>47</sup> as constructed previously<sup>44</sup> with a simple infection model of a 180-day exponentially distributed duration. The IRS component of the campaign consists of 70% of houses receiving IRS with a killing efficacy of 0.8 for indoor feeds. This coverage is repeated at one-year intervals, and the efficacy lasts one-year with box-shape durability for simplicity. The TBV component of the campaign performs mass vaccination every two years with 80% coverage and an initial efficacy of 0.9, decaying exponentially with a four-year time constant. The campaign is continued for ten years, and simulations are sorted based on whether they exhibit local elimination before campaign termination. The probability of elimination for the IRS campaign, mapping the probability of parasite persistence after ten years, is shown in Figure 6A. The horizontal axis scales the baseline vector population, which in turn approximately scales the EIR, except at low transmission levels, when the EIR decreases nonlinearly. A vector population scaling of 1.0 corresponds to actual baseline with an EIR of approximately 350 per year, with most caused by *An. arabiensis*. The vertical axis scales the propensity of *An. arabiensis* to feed indoors from 0 to 1. With the IRS only campaign, reliable elimination is only achieved in the upper left hand corner, corresponding to lower vector populations and higher indoor feeding, as expected. Even with all vectors feeding indoors, no simulations with a vector population scaling over 0.4 achieved elimination, although transmission was greatly reduced. With the TBV component added on (Figure 6B), the region of elimination expands, and campaigns that had limited transmission but could not fully interrupt it are assisted the most. Notably, the condition corresponding to baseline transmission with *An. arabiensis* resting outdoors after at least half of its feeds remains far from the region of elimination.

It seems clear that deployment of a vaccine is thus best accomplished in combination with a vector control intervention. Returning to the Namawala simulation with the full parasite microsolver, the results of studies shown in Figure 5

are repeated but now combined with vector control. Results for a 90% effective PEV (Figure 7A and B) and a 90% effective TBV (Figure 7C and D) deployed to Namawala as a standalone intervention, with a 70% coverage IRS campaign for *An. arabiensis* indoor feeding of 0.47, and with a 70% coverage IRS campaign for *An. arabiensis* indoor feeding of 0.7 are shown in Figure 7. For high indoor feeding, the IRS plus vaccine campaigns produce reductions in prevalence to < 10%, although transmission is not interrupted.

**Effect of intervention durability.** An important set of topics for modeling to address are the interrelationships among intervention efficacy, intervention durability, and the effects on parasite and vector dynamics. Sensitivity of the results of

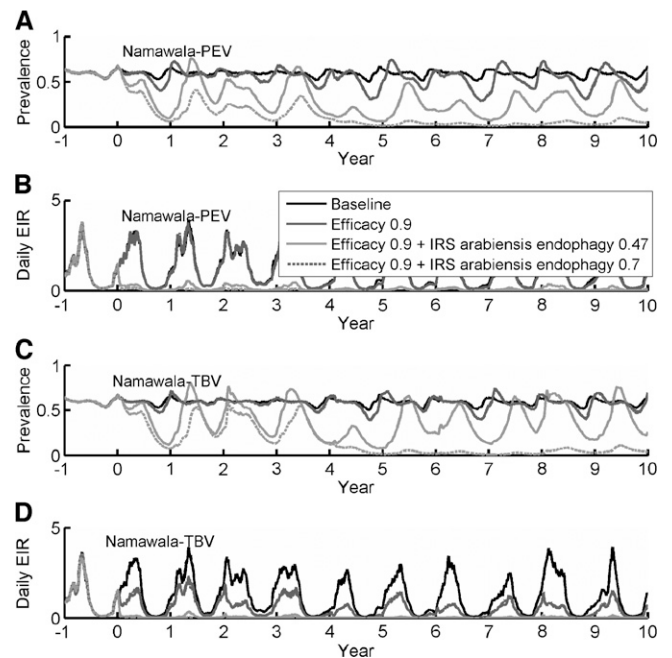


FIGURE 7. Effects of combining mass vaccination with vector control for pre-erythrocytic vaccine (PEV) (A and B) and sexual-stage transmission-blocking vaccine (TBV) (C and D) in Namawala, Tanzania. Baseline dynamics are presented with the vaccine by itself and the vaccine combined with 70% coverage with indoor residual spraying (IRS) for *Anopheles arabiensis* indoor feeding values of 0.47 and 0.7. EIR = entomologic inoculation rate.

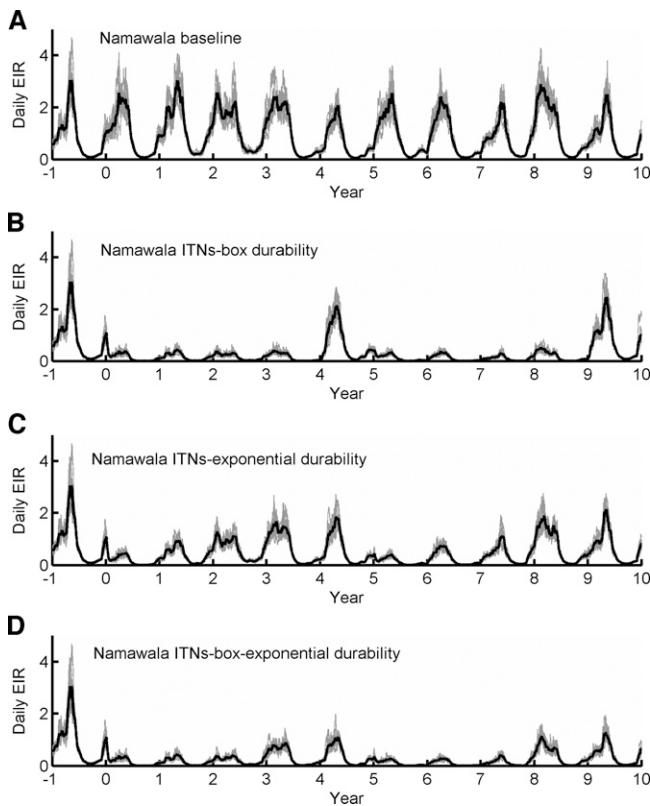


FIGURE 8. Efficacy decay profiles for insecticide-treated nets (ITNs) and effect on dynamics for Namawala, Tanzania dynamics and simple infection model. **A**, Baseline, no bed nets. **B**, ITNs distributed every five years with a four-year box efficacy. **C**, ITNs distributed every five years with an exponentially decaying efficacy with a four-year time constant. **D**, ITNs distributed every five years, with efficacy constant for two years, followed by exponential decay with a four-year time constant. EIR = entomologic inoculation rate.

a proposed campaign to intervention durability must be understood when planning repeated rounds of distributions and cost-effectiveness. Eleven years of dynamics for Namawala, Tanzania with the full vector model and the simple exponential-durations model for human infections are shown in Figure 8, with the ITN campaign starting after one year at time 0. Dynamics with no ITNs is shown in Figure 8A, and the year-to-year variability caused by rainfall patterns during 1990–1999<sup>68</sup> is clearly visible. Identical ITN campaigns, in which 70% of the population receives a new ITN every 5 years, are shown in Figure 8B–D. The ITNs are modeled to start with 100% efficacy at blocking attempted indoor feeds, and a 70% killing rate for blocked feeds. These efficacies are constant for four years, and then blocking and killing efficacies decrease to zero (Figure 8B). This feature results in a spike in the EIR in the fifth year before new ITNs are distributed the following year. The observed EIR for blocking and killing efficacies with both decaying exponentially with a time constant of four years is shown in Figure 8C. The decay in blocking efficacy further compounds the decay in killing efficacy, as would be expected when an ITN develops holes. These also resemble the dynamics one would expect if use of ITNs became increasingly sporadic over time. If the ITNs remain physically intact and able to block feeds indefinitely, then an exponential decay of the insecticide-killing effect is still

observed, but the controlled EIR does not increase as fast as shown in Figure 8C. An efficacy profile that maintains original efficacy for two years, followed by an exponential decay with a four-year time constant is shown in Figure 8D. Varying the intervention durability profile has dramatic effects on the system, illustrating that such sensitive input parameters must be well understood to achieve accurate model results.

## DISCUSSION

The EIR can vary significantly from year to year, even without changes in control, which complicates the essential task of monitoring for signs of slippage in control programs. The temporal dynamics of intervention efficacy are essential to consider when designing a campaign, and modeling can be used to specify the necessary frequencies of distribution, as well as to predict when one could expect to see increases in transmission caused by decay of interventions. The multiple efficacies of interventions are important to track because they may exhibit distinct temporal scales, with the physical integrity and insecticide concentrations of ITNs a classical example.

The reconstruction of the Garki Project demonstrates the ability of models to aid in the understanding of previous campaigns and in separating out hypotheses for the historical inability to interrupt transmission despite intense pressure. The level of transmission in the low-transmission season is a clear driver for the lack of seasonality in Namawala prevalence, in that the low-season transmission is not that low. However, in Garki, the low-transmission season had a much lower in EIR than that in Namawala, but extending spraying to a month before and a month after the rainy season has substantial impact in simulation, especially on the minimum prevalence experienced, which is important for fadeout. Careful modeling also illustrates the impact of assumptions on partition of the *An. gambiae* species complex. For a given level of indoor resting among the complex, it is more difficult to interrupt transmission with interventions that target indoor feeds if the component species are similar in baseline prevalence, which enable one component species to have minimal indoor resting and the other component species to balance the measured statistics in feeding location. This partition phenomenon has been noted and measured,<sup>66</sup> and the present results emphasize the importance for control programs of understanding and measuring these populations. In some studies, differences in insecticide-driven mortality has been observed across members of a species complex, even on a per-indoor-feed basis.<sup>69</sup> As interventions are introduced with different impacts on the local heterogeneous mix of vector species, the new proportions of transmission by species will change in simulation. This finding matches observations of changing epidemiology as ITN rollouts and other vector control campaigns have been conducted,<sup>5,6,12–14,62,63,70</sup> including such observations near Namawala.<sup>61</sup> The simulated impact of existing tools and new target product profiles for vector control will thus depend on the mixture of vector species, their ecologies, and their behaviors.

The Garki hypothetical extended campaign also demonstrates the potential role for new tools, such as vaccines when introduced to a campaign that has achieved dramatic reductions, but has run out of additional tools to introduce. The



Namawala simulations demonstrate how the impact of a vaccine depends on its efficacy, its duration of protection, and its mode and scale of distribution among the population. In addition, the strongest impacts are observed either at lower transmission levels, in which the linear effects of a vaccine can drive nonlinear decreases in transmission, or when combined with vector control that reduces baseline transmission. Thus, the local transmission intensity will affect vaccine rollout, as will the local vector behavior and ecology if combining with vector control. Simulations and analyses such as those in Figure 6 and Figure 7 can be used to define what a useful vaccine target profile will be in terms of efficacy, duration of protection, and ease of distribution. Simulations can also be used to prioritize rollout to where a vaccine will make the most relevant impacts. Various uncertainties around the potential impact of vaccines include the potential for immunotolerance driven by skin stages,<sup>71</sup> duration of protection, and strain specificity.

Mechanistic modeling can identify host and parasite factors that may impact the efficaciousness of control. Such factors identified in the detailed mechanistic model for parasite dynamics include gametocyte production and transmission,<sup>72</sup> antigenic variation,<sup>73</sup> and immune memory.<sup>74</sup> The local mixture of vector species and their ecologies and behaviors has a tremendous impact on the effect of introduced combinations of interventions, and current efforts to map these species ratios and measure these values are essential to inform planning.<sup>4,10,75,76</sup> Next steps for the current effort involve extending the model to mortality and severe disease and then estimating the effects of interventions on disease burden. Uncertain parameters to which the outcomes of simulated campaigns are sensitive can refine important research questions for field and laboratory studies, making modeling an essential tool in the research and planning of the global eradication campaign.<sup>41,77–79</sup>

Received January 4, 2012. Accepted for publication January 28, 2013.

Published online April 15, 2013.

**Acknowledgments:** I thank the Bill and Melinda Gates Foundation for their active support of this work and their sponsorship through the Global Good Fund. Useful discussions with colleagues at Intellectual Ventures Laboratory, the Malaria Program of the Bill and Melinda Gates Foundation, MalERA, and VECNet, especially Tom Burkot, Frank Collins, Neil Lobo, and Tanya Russell, are likewise greatly appreciated.

**Financial support:** This study was supported by the Bill and Melinda Gates Foundation through the Global Good Fund.

**Disclosure:** The author is employed by the Global Good Fund at Intellectual Ventures, LLC on a malaria modeling project. The models, software, and results will be freely available, so no financial or other conflict of interest exists. This statement is made in the interest of full disclosure and not because the author believes there is a conflict of interest.

**Author's address:** Philip Eckhoff, Intellectual Ventures Laboratory, Bellevue, WA, E-mail: peckhoff@intven.com.

## REFERENCES

1. Snow RW, Guerra CA, Noor AM, Myint HY, Hay SI, 2005. The global distribution of clinical episodes of *Plasmodium falciparum* malaria. *Nature* 434: 214–217.
2. World Health Organization, 2011. *World Malaria Report: 2011*. Geneva: World Health Organization.
3. Hay SI, Guerra CA, Gething PW, Patil AP, Tatem AJ, Noor AM, Kabaria CW, Manh BH, Elyazar IR, Brooker S, Smith DL, Moyeed RA, Snow RW, 2009. A world malaria map: *Plasmodium falciparum* endemicity in 2007. *PLoS Med* 6: e1000048.
4. Hay SI, Sinka ME, Okara RM, Kabaria CW, Mbithi PM, Tago CC, Benz D, Gething PW, Howes RE, Patil AP, Temperley WH, Bangs MJ, Chareonviriyaphap T, Elyazar IR, Harbach RE, Hemingway J, Manguin S, Mbogo CM, Rubio-Palis Y, Godfray HC, 2010. Developing global maps of the dominant *Anopheles* vectors of human malaria. *PLoS Med* 7: e1000209.
5. Gimnig JE, Kolczak MS, Hightower AW, Vulule JM, Schoute E, Kamau L, Phillips-Howard PA, Ter Kuile FO, Nahlen BL, Hawley WA, 2003. Effect of permethrin-treated bed nets on the spatial distribution of malaria vectors in western Kenya. *Am J Trop Med Hyg* 68: 115–120.
6. Gimnig JE, Vulule JM, Lo TQ, Kamau L, Kolczak MS, Phillips-Howard PA, Mathenge EM, ter Kuile FO, Nahlen BL, Hightower AW, Hawley WA, 2003. Impact of permethrin-treated bed nets on entomologic indices in an area of intense year-round malaria transmission. *Am J Trop Med Hyg* 68: 16–22.
7. Molineaux L, Gramiccia G, 1980. *The Garki Project: Research on the Epidemiology and Control of Malaria in the Sudan Savanna of West Africa*. Geneva: World Health Organization.
8. Romi R, Razaarimanga MC, Raharimanga R, Rakotondraibe EM, Ranaivo LH, Pietra V, Raveloson A, Majori G, 2002. Impact of the malaria control campaign (1993–1998) in the highlands of Madagascar: parasitological and entomological data. *Am J Trop Med Hyg* 66: 2–6.
9. Killeen G, Fillinger U, Knols B, 2002. Advantages of larval control for African malaria vectors: low mobility and behavioural responsiveness of immature mosquito stages allow high effective coverage. *Malar J* 1: 8.
10. Fillinger U, Sonye G, Killeen GF, Knols B, Becker N, 2004. The practical importance of permanent and semipermanent habitats for controlling aquatic stages of *Anopheles gambiae* sensu lato mosquitoes: operational observations from a rural town in western Kenya. *Trop Med Int Health* 9: 1274–1289.
11. Fillinger U, Kannady K, William G, Vanek M, Dongus S, Nyika D, Geissbuhler Y, Chaki P, Govella N, Mathenge E, Singer B, Mshinda H, Lindsay S, Tanner M, Mtsiwa D, de Castro M, Killeen G, 2008. A tool box for operational mosquito larval control: preliminary results and early lessons from the urban malaria control programme in Dar es Salaam, Tanzania. *Malar J* 7: 20.
12. Reddy M, Overgaard H, Abaga S, Reddy V, Caccone A, Kiszewski A, Slotman M, 2011. Outdoor host seeking behaviour of *Anopheles gambiae* mosquitoes following initiation of malaria vector control on Bioko Island, Equatorial Guinea. *Malar J* 10: 184.
13. Bugoro H, Iro'ofa C, Mackenzie D, Apairamo A, Hevalao W, Corcoran S, Bobogare A, Beebe N, Russell T, Chen C-C, Cooper R, 2011. Changes in vector species composition and current vector biology and behaviour will favour malaria elimination in Santa Isabel Province, Solomon Islands. *Malar J* 10: 287.
14. Derua Y, Alifrangis M, Hosea K, Meyrowitsch D, Magea S, Pedersen E, Simonsen P, 2012. Change in composition of the *Anopheles gambiae* complex and its possible implications for the transmission of malaria and lymphatic filariasis in north-eastern Tanzania. *Malar J* 11: 188.
15. Okell LC, Drakeley CJ, Bousema T, Whitty CJ, Ghani AC, 2008. Modelling the impact of artemisinin combination therapy and long-acting treatments on malaria transmission intensity. *PLoS Med* 5: e226.
16. von Seidlein L, Greenwood BM, 2003. Mass administrations of antimalarial drugs. *Trends Parasitol* 19: 452–460.
17. Khatib R, Skarbinski J, Njau J, Goodman C, Elling B, Kahigwa E, Roberts J, MacArthur J, Gutman J, Kabanyanyi A, Smith E, Soti M, Lyimo T, Mwita A, Genton B, Tanner M, Mills A, Mshinda H, Bloland P, Abdulla S, Kachur S, 2012. Routine delivery of artemisinin-based combination treatment at fixed health facilities reduces malaria prevalence in Tanzania: an observational study. *Malar J* 11: 140.
18. Huho B, Killeen G, Ferguson H, Tami A, Lengeler C, Charlwood JD, Kihonda A, Kihonda J, Kachur SP, Smith T, Abdulla S, 2012. Artemisinin-based combination therapy does not measurably reduce human infectiousness to vectors in a setting of intense malaria transmission. *Malar J* 11: 118.

19. Shekalaghe S, Drakeley C, van den Bosch S, ter Braak R, van den Bijllaardt W, Mwanziva C, Semvua S, Masokoto A, Moshia F, Teelen K, Hermsen R, Okell L, Gosling R, Sauerwein R, Bousema T, 2011. A cluster-randomized trial of mass drug administration with a gametocytocidal drug combination to interrupt malaria transmission in a low endemic area in Tanzania. *Malar J* 10: 247.
20. Penny MA, Maire N, Studer A, Schapira A, Smith TA, 2008. What should vaccine developers ask? Simulation of the effectiveness of malaria vaccines. *PLoS ONE* 3: e3193.
21. RTS SCTP, 2012. A phase 3 trial of RTS,S/AS01 malaria vaccine in African infants. *N Engl J Med* 367: 2284–2295.
22. De Castro MC, Yamagata Y, Mtasiwa D, Tanner M, Utzinger J, Keiser J, Singer BH, 2004. Integrated urban malaria control: a case study in Dar es Salaam, Tanzania. *Am J Trop Med Hyg* 71: 103–117.
23. McKenzie FE, Baird JK, Beier JC, Lal AA, Bossert WH, 2002. A biologic basis for integrated malaria control. *Am J Trop Med Hyg* 67: 571–577.
24. Killeen G, McKenzie F, Foy B, Schieffelin C, Billingsley P, Beier J, 2000. The potential impact of integrated malaria transmission control on entomologic inoculation rate in highly endemic areas. *Am J Trop Med Hyg* 62: 545–551.
25. Fillinger U, Ndenga B, Githeko A, Lindsay SW, 2009. Integrated malaria vector control with microbial larvicides and insecticide-treated nets in western Kenya: a controlled trial. *Bull World Health Organ* 87: 655–665.
26. Macdonald G, 1956. Theory of the eradication of malaria. *Bull World Health Organ* 15: 369–387.
27. Macdonald G, 1957. *The Epidemiology and Control of Malaria*. London: Oxford University Press.
28. Ross R, 1910. *The Prevention of Malaria*. London: J. Murray.
29. Garrett-Jones C, 1964. Prognosis for interruption of malaria transmission through assessment of the mosquito's vectorial capacity. *Nature* 204: 1173–1175.
30. Depinay J-M, Mbogo C, Killeen G, Knols B, Beier J, Carlson J, Dushoff J, Billingsley P, Mwambi H, Githure J, Toure A, Ellis McKenzie F, 2004. A simulation model of African *Anopheles* ecology and population dynamics for the analysis of malaria transmission. *Malar J* 3: 29.
31. Bombliès A, Duchemin J-B, Eltahir E, 2009. A mechanistic approach for accurate simulation of village scale malaria transmission. *Malar J* 8: 223.
32. Okell L, Drakeley C, Ghani A, Bousema T, Sutherland C, 2008. Reduction of transmission from malaria patients by artemisinin combination therapies: a pooled analysis of six randomized trials. *Malar J* 7: 125.
33. Maude R, Pontavornpinyo W, Saralamba S, Aguas R, Yeung S, Dondorp A, Day N, White N, White L, 2009. The last man standing is the most resistant: eliminating artemisinin-resistant malaria in Cambodia. *Malar J* 8: 31.
34. Boni MF, Smith DL, Laxminarayan R, 2008. Benefits of using multiple first-line therapies against malaria. *Proc Natl Acad Sci USA* 105: 14216–14221.
35. Ross A, Penny M, Maire N, Studer A, Carneiro I, Schellenberg D, Greenwood B, Tanner M, Smith T, 2008. Modelling the epidemiological impact of intermittent preventive treatment against malaria in infants. *PLoS ONE* 3: e2661.
36. Smith T, Killeen GF, Maire N, Ross A, Molineaux L, Tediosi F, Hutton G, Utzinger J, Dietz K, Tanner M, 2006. Mathematical modeling of the impact of malaria vaccines on the clinical epidemiology and natural history of *Plasmodium falciparum* malaria: overview. *Am J Trop Med Hyg* 75: 1–10.
37. Tediosi F, Hutton G, Maire N, Smith TA, Ross A, Tanner M, 2006. Predicting the cost-effectiveness of introducing a pre-erythrocytic malaria vaccine into the expanded program on immunization in Tanzania. *Am J Trop Med Hyg* 75: 131–143.
38. Struchiner CJ, Halloran ME, Spielman A, 1989. Modeling malaria vaccines. I: new uses for old ideas. *Math Biosci* 94: 87–113.
39. Smith T, Maire N, Ross A, Penny M, Chitnis N, Schapira A, Studer A, Genton B, Lengeler C, Tediosi F, De Savigny D, Tanner M, 2008. Towards a comprehensive simulation model of malaria epidemiology and control. *Parasitology* 135: 1507–1516.
40. Griffin JT, Hollingsworth TD, Okell LC, Churcher TS, White M, Hinsley W, Bousema T, Drakeley CJ, Ferguson NM, Basáñez M-G, Ghani AC, 2010. Reducing *Plasmodium falciparum* malaria transmission in Africa: a model-based evaluation of intervention strategies. *PLoS Med* 7: e1000324.
41. Alonso PL, Brown G, Arevalo-Herrera M, Binka F, Chitnis C, Collins F, Doumbo OK, Greenwood B, Hall BF, Levine MM, Mendis K, Newman RD, Plowe CV, Rodríguez MH, Sinden R, Slutsker L, Tanner M, 2011. A research agenda to underpin malaria eradication. *PLoS Med* 8: e1000406.
42. The mal ERACGoM, 2011. A research agenda for malaria eradication: modeling. *PLoS Med* 8: e1000403.
43. Smith T, Ross A, Maire N, Chitnis N, Studer A, Hardy D, Brooks A, Penny M, Tanner M, 2012. Ensemble modeling of the likely public health impact of a pre-erythrocytic malaria vaccine. *PLoS Med* 9: e1001157.
44. Eckhoff P, 2011. A malaria transmission-directed model of mosquito life cycle and ecology. *Malar J* 10: 303.
45. Eckhoff P, 2012. *P. falciparum* infection durations and infectiousness are shaped by antigenic variation and innate and adaptive host immunity in a mathematical model. *PLoS ONE* 7: e44950.
46. Smith DL, McKenzie FE, 2004. Statics and dynamics of malaria infection in *Anopheles* mosquitoes. *Malar J* 3: 13.
47. Smith T, Charlwood JD, Kihonda J, Mwankusye S, Billingsley P, Meuwissen J, Lyimo E, Takken W, Teuscher T, Tanner M, 1993. Absence of seasonal variation in malaria parasitaemia in an area of intense seasonal transmission. *Acta Trop* 54: 55–72.
48. Eckhoff P, 2012. Malaria parasite diversity and transmission intensity affect development of parasitological immunity in a mathematical model. *Malar J* 11: 419.
49. Seyoum A, Sikaala C, Chanda J, Chinula D, Ntamatungiro A, Hawela M, Miller J, Russell T, Briet OJ, Killeen G, 2012. Human exposure to anopheline mosquitoes occurs primarily indoors, even for users of insecticide-treated nets in Luangwa Valley, south-east Zambia. *Parasit Vectors* 5: 101.
50. Kiwara SS, Chitnis N, Devine GJ, Moore SJ, Majambere S, Killeen GF, 2012. Biologically meaningful coverage indicators for eliminating malaria transmission. *Biol Lett* 8: 874–877.
51. Recker M, Nee S, Bull PC, Kinyanjui S, Marsh K, Newbold C, Gupta S, 2004. Transient cross-reactive immune responses can orchestrate antigenic variation in malaria. *Nature* 429: 555–558.
52. Fowkes FJ, Richards JS, Simpson JA, Beeson JG, 2010. The relationship between anti-merozoite antibodies and incidence of *Plasmodium falciparum* malaria: a systematic review and meta-analysis. *PLoS Med* 7: e1000218.
53. Lengeler C, 2004. Insecticide-treated nets for malaria control: real gains. *Bull World Health Organ* 82: 84–84.
54. Pluess B, Tanser Frank C, Lengeler C, Sharp Brian L, 2010. *Indoor Residual Spraying for Preventing Malaria*. Cochrane Database of Systematic Reviews. New York: John Wiley & Sons, Ltd.
55. Smith T, Maire N, Dietz K, Killeen GF, Vounatsou P, Molineaux L, Tanner M, 2006. Relationship between the entomologic inoculation rate and the force of infection for *Plasmodium falciparum* malaria. *Am J Trop Med Hyg* 75: 11–18.
56. Collins WE, Jeffery GM, 1999. A retrospective examination of sporozoite- and trophozoite-induced infections with *Plasmodium falciparum*: development of parasitologic and clinical immunity during primary infection. *Am J Trop Med Hyg* 61: 4–19.
57. Recker M, Buckee CO, Serazin A, Kyes S, Pinches R, Christodoulou Z, Springer AL, Gupta S, Newbold CI, 2011. Antigenic variation in *Plasmodium falciparum* malaria involves a highly structured switching pattern. *PLoS Pathog* 7: e1001306.
58. Maire N, Smith T, Ross A, Owusu-Agyei S, Dietz K, Molineaux L, 2006. A model for natural immunity to asexual blood stages of *Plasmodium falciparum* malaria in endemic areas. *Am J Trop Med Hyg* 75: 19–31.
59. Garki, 2011. *The Garki Portal*. Available at: rhgarki.crc.nd.edu. Accessed February 7, 2013.
60. Govella NJ, Okumu FO, Killeen GF, 2010. Insecticide-treated nets can reduce malaria transmission by mosquitoes which feed outdoors. *Am J Trop Med Hyg* 82: 415–419.
61. Russell T, Govella N, Azizi S, Drakeley C, Kachur SP, Killeen G, 2011. Increased proportions of outdoor feeding among

- residual malaria vector populations following increased use of insecticide-treated nets in rural Tanzania. *Malar J* 10: 80.
62. Bejon P, Williams TN, Liljander A, Noor AM, Wambua J, Ogada E, Olotu A, Osier FH, Hay SI, Färnert A, Marsh K, 2010. Stable and unstable malaria hotspots in longitudinal cohort studies in Kenya. *PLoS Med* 7: e1000304.
  63. Bousema T, Griffin JT, Sauerwein RW, Smith DL, Churcher TS, Takken W, Ghani A, Drakeley C, Gosling R, 2012. Hitting hotspots: spatial targeting of malaria for control and elimination. *PLoS Med* 9: e1001165.
  64. Charlwood JD, Vij R, Billingsley PF, 2000. Dry season refugia of malaria-transmitting mosquitoes in a dry savannah zone of east Africa. *Am J Trop Med Hyg* 62: 726–732.
  65. Coluzzi M, Sabatini A, Petrarca V, Angela Di Deco M, 1977. Behavioural divergences between mosquitoes with different inversion karyotypes in polymorphic populations of the *Anopheles gambiae* complex. *Nature* 266: 832–833.
  66. Coluzzi M, Sabatini A, Petrarca V, Di Deco MA, 1979. Chromosomal differentiation and adaptation to human environments in the *Anopheles gambiae* complex. *Trans R Soc Trop Med Hyg* 73: 483–497.
  67. Kulkarni MA, Desrochers RE, Kerr JT, 2010. High resolution niche models of malaria vectors in northern Tanzania: a new capacity to predict malaria risk? *PLoS ONE* 5: e9396.
  68. Centre GPC, 2008. *Full Data Reanalysis*. Available at: <http://gpcc.dwd.de>. Accessed 2008.
  69. Kitau J, Oxborough RM, Tungu PK, Matowo J, Malima RC, Magesa SM, Bruce J, Mosha FW, Rowland MW, 2012. Species shifts in the *Anopheles gambiae* complex: do LLINs successfully control *Anopheles arabiensis*? *PLoS ONE* 7: e31481.
  70. Ferguson H, Maire N, Takken W, Lyimo I, Briet O, Lindsay S, Smith T, 2012. Selection of mosquito life-histories: a hidden weapon against malaria? *Malar J* 11: 106.
  71. Guilbride DL, Patrick DL, Pawel PG, 2012. Malaria's deadly secret: a skin stage. *Trends Parasitol* 28: 142–150.
  72. Drakeley C, Sutherland C, Bousema JT, Sauerwein RW, Targett GA, 2006. The epidemiology of *Plasmodium falciparum* gametocytes: weapons of mass dispersion. *Trends Parasitol* 22: 424–430.
  73. Bull PC, Lowe BS, Kortok M, Molyneux CS, Newbold CI, Marsh K, 1998. Parasite antigens on the infected red cell surface are targets for naturally acquired immunity to malaria. *Nat Med* 4: 358–360.
  74. Langhorne J, Ndungu FM, Sponaas AM, Marsh K, 2008. Immunity to malaria: more questions than answers. *Nat Immunol* 9: 725–732.
  75. Killeen GF, McKenzie FE, Foy BD, Bogh C, Beier JC, 2001. The availability of potential hosts as a determinant of feeding behaviours and malaria transmission by African mosquito populations. *Trans R Soc Trop Med Hyg* 95: 469–476.
  76. Graves PM, Burkot TR, Saul AJ, Hayes RJ, Carter R, 1990. Estimation of anopheline survival rate, vectorial capacity and mosquito infection probability from malaria vector infection rates in villages near Madang, Papua New Guinea. *J Appl Ecol* 27: 134–147.
  77. Cohen JM, Smith DL, Valley A, Taleo G, Malefoasi G, Sabot O, 2009. Holding the line. Feachem RG, Phillips AA, Targett GA, Group ME, eds. *Shrinking the Malaria Map: A Prospectus on Malaria Elimination*. San Francisco, CA: The Global Health Group: UCSF Global Health Sciences, 40–60.
  78. Moonen B, Barrett S, Tulloch J, Jamison DT, 2009. Making the decision. Feachem RG, Phillips AA, Targett GA, Group ME, eds. *Shrinking the Malaria Map: A Prospectus on Malaria Elimination*. San Francisco, CA: The Global Health Group: UCSF Global Health Sciences, 1–18.
  79. Smith DL, Smith TA, Hay SI, 2009. Measuring malaria for elimination. Feachem RG, Phillips AA, Targett GA, Group ME, eds. *Shrinking the Malaria Map: A Prospectus on Malaria Elimination*. San Francisco, CA: The Global Health Group: UCSF Global Health Sciences, 108–126.